# Fracture Growth on Långören Island, Finland, on the Hottest Day on Record in 2014

Alcaino-Olivares, R., Hayden, D., Perras, M.A.*
*Department of Civil Engineering, York University, Toronto, Ontario, Canada*
Leith, K., Loew, S.
*Engineering Geology Group, ETHZ, Zurich, Switzerland**

## ABSTRACT

Observations on the hottest day in Finland have shown the potential effect on crack growth. The current research presents a site investigation on Långören Island (Finland) where acoustic emission, crack meter and weather parameters including air and rock temperature sensors were installed. In addition, laboratory tests for Indirect Tensile Strength and P-wave velocity were conducted. Results suggest that large temperature variations are affecting the shallow layer of the rock surface. Laboratory tests indicate a variation in P-wave velocity at different orientations, suggesting that anisotropy could be the result of preferred micro-cracks orientations. Ongoing data collection and correlations between crack growth and the climatic variables will help improve our understanding of the crack growth mechanism.

## RÉSUMÉ

Les observations sur le jour le plus chaud en Finlande ont montré l'effet potentiel sur la croissance des fissures. Cette recherche présente une étude de site sur l'île de Långören (Finlande) où des capteurs d'émission acoustique, de débitmètre et de météorologie, y compris des capteurs de température de l'air et de la roche, ont été installés. De plus, des tests de laboratoire de résistance à la traction indirecte et de vitesse de l'onde P ont été effectués. Les résultats mettent en évidence les grandes variations de température qui affectent la couche peu profonde de la roche. Les tests de laboratoire indiquent une variation de la vitesse de l'onde P suivant plusieurs directions de propagation, suggérant que l'anisotropie pourrait être le résultat des choix sur l'orientation des micro-fissures. La collecte continue de données et la corrélation entre la croissance des fissures et les variables climatiques aideront à améliorer notre compréhension du mécanisme de croissance des fissures.

## 1 INTRODUCTION

The effect of temperature on the response of cracks in materials has been widely analyzed by many authors in various contexts including, material science, civil engineering projects, mechanical engineering, and electrical devices (Sih & DiTommaso, 1985; Abeka et al., 2017). In geological materials, the effect of thermal expansion of rocks and rock masses is variable since the geological units vary at multiple scales (grains, veins, formations). Various studies have been conducted to understand how rocks are affected by thermal processes and gain knowledge for engineering applications, such as underground nuclear waste storage facilities (Huan et al., 2017; Jansen & Carlson et al., 1993). Thermodynamic models help develop a better understanding of how the energy given by heat flow and the response of rocks through thermal strain are related (Rice, 1977; Cooper & Simons, 1977).

In addition to the inherent variability of rock masses, the added challenge of large-scale geological features, such as faults or folds, will also influence crack growth in the rock mass. Therefore, it may be difficult to isolate in-situ thermal effects from other influences. In fact, the lack of direct observations of natural cracking events driven by environmental factors has made it problematic to determine a precise mechanism for crack growth and thermal fracturing at the rock mass scale (Collins et al., 2018).

However, conceptually heat transfer and thermal effects can play a key role in the stability of natural landscapes, civil engineering infrastructure, or the rock mass in general, with the consequences being reported by many authors (e.g. Vlcko et al., 2008; Lamp et al., 2016; Hall & Andre, 2001; Grief et al., 2005; Bakun-Mazore et al., 2013).

Collins & Stock (2016) claim that cyclic variation of temperature guides opening and closing sequences of fractures, which may lead to rock falls associated with solar radiation in combination with gravity. Additionally, Collins et al. (2018) have reported natural cracking events of spontaneous exfoliation and crack propagation during extremely hot periods in the granitic dome at the Twain Harte Dam site, California, USA, in the summer of 2014. The observations showed that thermal stresses could be an important agent to shape domes and produce exfoliation. Their publication contains a well-documented dynamic response of the rock mass, observed in 2014 and subsequently accompanied by various measurements starting in late 2014.

Similarly, during extremely hot temperatures in the summer of 2014, a dynamic cracking event was also recorded by video on Långören Island in the Archipelago Sea of Finland (see Figure 1). The rock mass of this island is a meta-granite, with a shallow dome curvature. The fractures here are also consistent with exfoliation type fractures containing characteristic sharp edges and forming thin sheets of rock parallel to the ground surface (Figure 2).

In 2014 and 2015 researchers investigated the events on Långören Island and in 2016 instrumentation was installed (Leith et al. 2017). Further detailed were also gathered during the instrumentation installation to support inputs into a fracture mechanics model of the site. Rantanen (2016) simulated the exfoliation of the rock mass focused on three influencing factors: topography, post-glacial up-lifting, and long-term (weekly) and daily thermal expansion; concluding that thermal expansion was the most important triggering agent in combination with high horizontal stresses.

The above investigations have prompted continued study of the site to determine the role of climatic variables on driving fracture growth on Långören Island. The details of the geological environment, installation of instruments, and analysis of laboratory measurements are presented in this paper.

## 2 CHARACTERISTICS OF LÅNGÖREN ISLAND

### 2.1 Geological Setting

Långören Island is part of the Archipelago Sea of Finland, which is composed of over 20,000 small islands. The Archipelago is located at the edge of the Gulf of Bothnia and the Gulf of Finland, covering 8,000 km$^2$. The bedrock of the archipelago consists of igneous and metamorphic rocks from the Svecofennian orogeny (Proterozoic era), in association with interbeds of calcareous features from supracrustal units. The geological domain of Långören Island is defined by Edelman (1960) as a microcline granite (see Figure 1), formed through granitization processes during metamorphism in the last stage of the orogenic evolution. The modes of granitization vary by composition and structure of the primary rocks (Edelman, 1960), forming domes possibly due to the plastic behaviour of the primary rocks (Virtasalo, 2006; Paulamaki et al., 2002; Edelman & Jaanus-Järkkälä, 1983).

The geological evolution of the area includes a series of folding and fracturing (joint formation) processes, along with intrusive activities during the Svecofennian period. The geological evolution resulted in migmatites, magmatic granites, pegmatites, crystalline schist, and alkali-calcic igneous rocks, along with amphibolite dikes developed in a series of folds in the region. The geological units were significantly eroded during the Cambrian era close to the current elevation (Edelman, 1960; Edelman & Jaanus-Järkkälä, 1983).

The region was severely affected by ice loading during the last glaciation in the Holocene. The ice loading increased the vertical load, causing crustal deformation. Up-lift due to glacial isostatic adjustment continues today with local up-lift rates near Långören Island in the range of 4-8 mm/a (Johannsson et al., 2002; Poutanen et al., 2010).

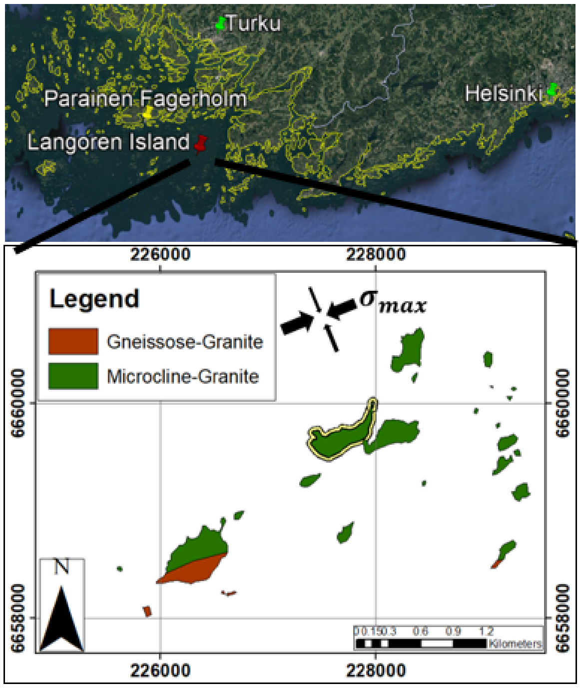

Figure 1. Location of Långören Island (red pin & outlined) and the local geologic units (modified from Edelman 1960).

Figure 2. Observed fractures from the summer of 2014 (pictures courtesy of Mr. Sarpaneva).

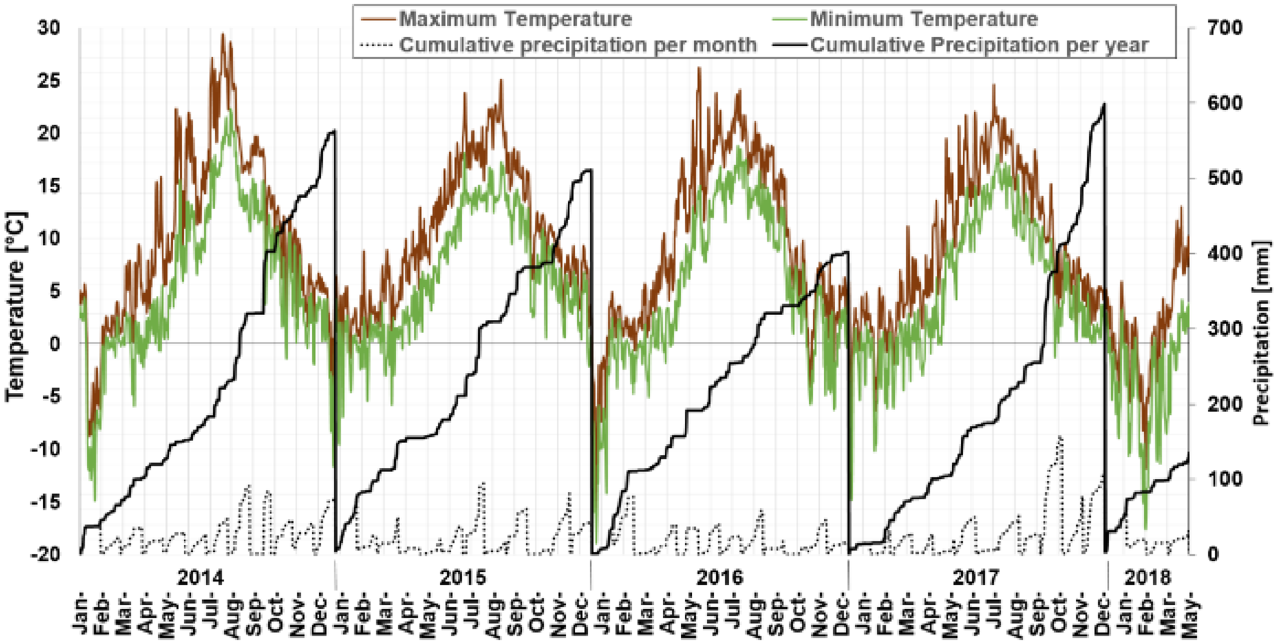

Figure 3: Regional values for temperature and precipitation at Långören Island, taken from the Finnish Meteorological Institute for Paranein Fagerholm weather station. Values are plotted from January 2014 to May 2018.

A series of melting stages of the Fennoscandian ice-sheet since 14.000 BP have influenced the quaternary deposits, washing the sediments to the sea bottom. As the sea level rose the paleo-Baltic Ice Lake was connected with the North Sea. This allowed salt water infiltration and shaped the current sea conditions (Virtasalo, 2006; Granö et al., 1999).

The glacial processes polished the rock surface, washed the weathered products, and exposed the current bedrock surface along with the structural features (Virtasalo, 2006).

## 2.2 Geotechnical Setting

The assumed major principal horizontal stress in the region is orientated NE-SW, taken from the closest measurements in Turku (Pennala, 2017). The magnitude of the major horizontal stress ranges from 7 to 13 MPa and the minor stress from 3 to 7 MPa, between 10-20 m depth.

Seismic activity recorded since 1610 has shown that no earthquakes greater than Mw 5 have been recorded (Ahjos et al., 1984). However, predictions of earthquakes with no historical magnitude limit indicate that a maximum of Mw 7.9 could be reached near Långören Island (Saari, 2000).

Rantanen (2016) reported that the geotechnical properties of the microcline granite display similar characteristics to that of the Olkiluoto granite. The main values reported for the intact rock include a uniaxial compression strength (UCS) of 115 MPa, Young's modulus (E) of 55 GPa, Poisson's ratio ($\nu$) of 0.2, and tensile strength ($\sigma_t$) of 12 MPa. In addition, Rantanen (2016) also reports a coefficient of thermal expansion, $b_t$, of 9.0x10$^{-6}$ mm/mm°C, thermal conductivity, $c_t$, of 3.2 W/mK, and a specific heat capacity, $c_p$, of 689 J/kgK.

## 2.3 Hydrogeological and Climatic Settings

In the larger regional area, the sea can be divided into several channels which connect the central and northern part of the Baltic Sea. These are fed by fluvial discharge from the mainland contributing to sediment accumulation on the seabed (Kaskela, 2017).

Locally, the western part of the island is an exposed bedrock dome that transitions to a vegetated spit in the northeastern region (Figure 1). Surfaces runoff flows over the bedrock surface or infiltrates the thin rocky soil cover. There are no streams or ponds on the island. The only trace of standing surface water includes shallow pools that are present after heavy rainfall and evaporate over time as the water cannot infiltrate the rock mass.

The climate displays large seasonal variations, having a wide range of extreme temperatures during winter and summer (Figure 3). Temperatures higher than the historic summer mean value of 18°C have been recorded in July and August over the last 4 years between 25°C to 30°C. The maximum temperatures every recorded to date were in the summer of 2014. An observation from the precipitation indicates that there was less cumulative yearly rain in July 2014 than subsequent summers (Figure 3).

Långören Island is located in the region that receives the highest rates of radiation in Finland (Rantanen, 2016). Climate change during the last century has raised the sea level, air temperature, the amount of precipitation, and the wind speed. The combined changes in the climate may have caused a decrease in the salinity of the sea (Jokinsen, 2010), contributing to potential changes in the rock mass in the near surface.

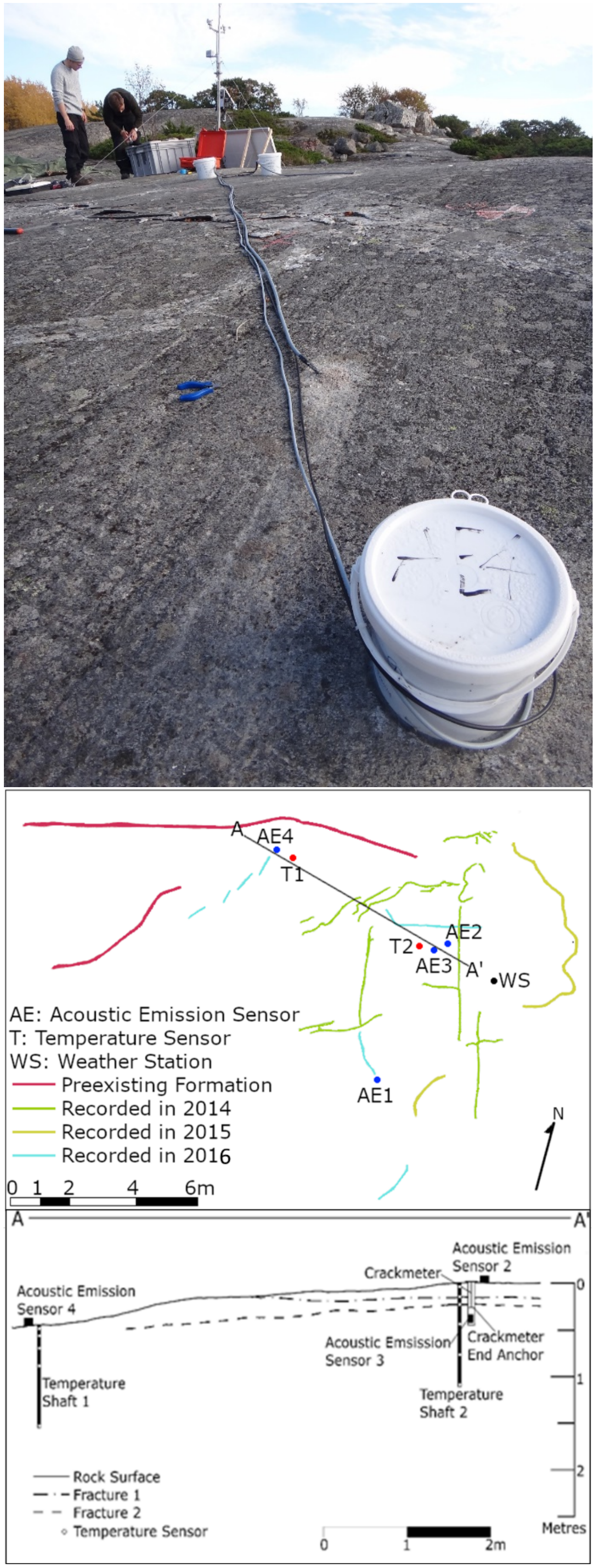

Figure 4: A picture of the installed system (top) and the location of instrumentation and fractures on Långören Island (plan view middle and cross section bottom).

# 3 DESIGNING THE MONITORING SYSTEM

## 3.1 Considerations

In late 2015, an instrumentation plan was developed for Långören Island to monitor existing fracture behavior and identify new fractures. During the planning stages, photos and mapping (from 2014 & 2015) of the fractured zone (Figure 4) were used.

The existing information indicated that a near surface fracture created a slab of rock free on three sides. The slab appeared to maintain connection to the rock mass on the west end (Figure 4). This upper slab was targeted for monitoring movement that would be correlated with environmental variables. The movement of the existing slab and growth of existing fractures was deemed to be the critical element of the monitoring system. A crack meter only monitors one location, so it was decided that a micro-seismic or acoustic emission (AE) system would also be deployed to capture new fracturing of intact rock and breaking of asperities during movement of existing fractures. In addition, the climatic variables and the rock temperature gradients were included in the monitoring system.

To measure the movement of the slab via a crack meter a borehole passing across the near surface fractures was planned. The crack meter designed to be anchored in the rock below the fracture thereby allowing the vertical motion of the slab to be monitored. In addition, a down borehole AE sensor mount was designed to monitor activity below the surface (see Figure 4). To ensure optimum anchoring to the borehole wall, coring was considered with the added benefit of yielding samples for testing in the laboratory. Boreholes were also planned for the rock temperature gradient monitoring system. However, a destructive hammer drill was considered rather than a coring machine due to the depth requirements and time constraints. Two temperature gradient strings were planned; one that crossed through the upper slab and one that was drilled off the slab such that it did not intersect the upper slab. This was done to understand the influence of fracture on the rock temperature gradient. Finally, a weather station was needed to make correlations between the thermal-mechanical measurements and the climatic variables. The weather station selected could measure the wind speed and direction, precipitation, air temperature, humidity, pressure, solar radiation, luminosity, and the rock surface temperature. These components were all installed in July 2016 (see Figure 4 for relative position to the fractures).

## 3.2 Instrumentation Details

The crack movement and climatic variables were monitored with a Libelium Plug and Sense Agriculture Pro station which included a weather station and a crack meter. The station was situated on a mast and the crack meter was associated with the cored borehole (see Figure 4). The crack meter was placed at the ground surface and an anchor placed at the bottom of the borehole below two near surface fractures (see core sample in Figure 5). The system logs the data locally, separate from the AE and temperature string systems.

The AE system consisted of four sensors with a resonance frequency of 60 kHz and built in 26 dB pre-amplifiers. These sensors are contained in housing that intends to minimize the effects of both radio frequency and electromagnetic interference. Plastic containers were placed over the sensors and filled with sand to eliminate noise from exterior sources, such as wind or direct rain impact. The sensors were glued and anchored directly to exposed bedrock. Three were placed at the surface – two on top of the slab and one off the slab near the tip of the 2014 fracture. The surface was ground flat before gluing to eliminate air pockets between the sensor and the rock. The location of these sensors is shown in Figure 4. The system was connected to a field computer running AE data acquisition system. The system was installed in trigger mode to capture the waveform whenever an event was detected. The field computer stored the data locally for the AE system and the temperature gradient strings.

The temperature gradient strings were custom made using PT 1000 temperature sensors and an Arduino microcontroller for data acquisition. The data was accumulated on the field computer. The sensors were placed at 0.04, 0.15, 0.23, 0.44, 0.77, and 1.11 m below the ground surface in two boreholes. The boreholes were filled with coarse aggregate grout to have similar thermal properties to the rock. The temperature sensors were read once every 200 seconds.

This network of sensors was monitored remotely during the summer of 2016 via 4G connection. However, during limited sunlight in the winter, the battery packs were considered to be insufficient at powering the entire system. The AE system was removed in September 2016 to conserve battery life and continue datalogging the weather station, crack meter, and temperature gradient data through the winter.

## 4 PRELIMINARY DATA ANALYSIS

### 4.1 Laboratory Tests

Several hand samples and a core sample were collected, as shown in Figure 5. The core sample was 321 mm in length and had a diameter of 69.3 mm. This was the only cored sample that could be taken from the island. Additionally, one of the hand samples was suitable for Brazilian tensile testing, also shown in Figure 5. These samples were used to measure the tensile strength ($\sigma_t$) and P-wave velocity values with depth and orientation. Sub-samples were taken perpendicular to the major axis of the sample (A axis), using two samples per sub-coring. Two fractures were identified in the cored samples which are visible at 150 mm and 210 mm depth below surface (Figure 5). These represent the fractures that propagated on the hottest day recorded at the site.

Brazilian indirect tensile tests were conducted according the ISRM (1978) suggested methods. The A axis samples were tested such that the tensile fracture would be induced parallel to the ground surface. According to Hoek and Martin (2014), there should be longer micro cracks, Griffith flaws, and tensile wing cracks in the horizontal plane than the vertical plane, due to the high horizontal stresses in the near surface. Depending on the micro crack density, the rock mass could be weaker in the near surface than at depth leading to a strength anisotropy.

In order to test the influence of micro-crack orientation on the strength indirect Brazilian tensile tests and P-wave velocity measurements were conducted. The tensile tests were done to induced tensile cracks parallel or perpendicular to the ground surface and those orientations were also used to measure P-wave velocity.

Although there were a limited number of samples, the average A axis tensile strength is 14.3 MPa and the B axis is 12.3 MPa (see inset table in Figure 5). Generally, the surface hand sample tensile strengths are lower than those from the core sample, regardless of orientation. In fact, the average value for the tensile strength of the hand sample, 10.9 MPa, is less than the minimum value of the core sample (C1.2.2: 13.6 MPa), regardless of orientation.

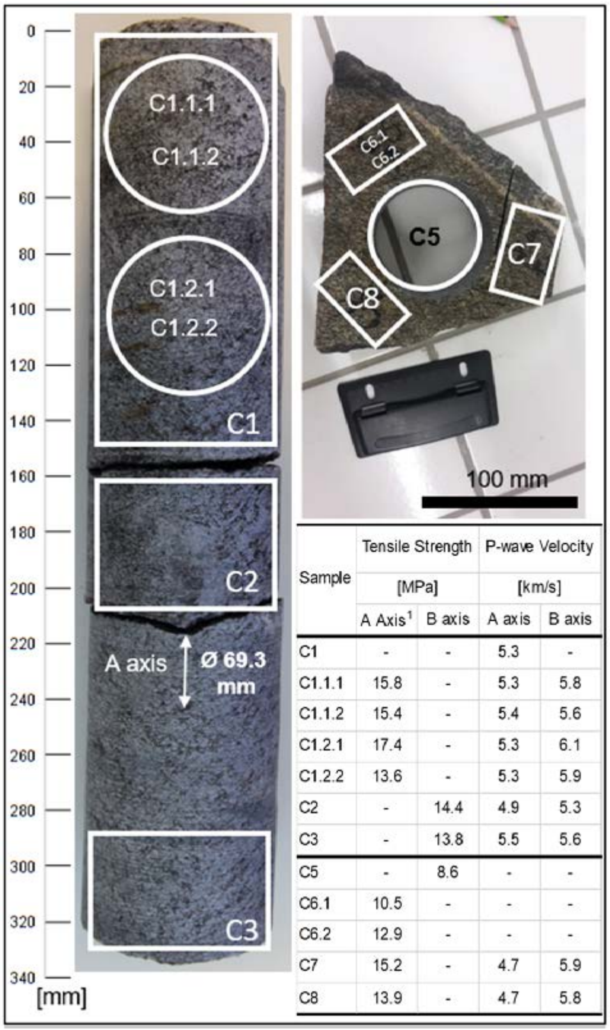

| Sample | Tensile Strength [MPa] | | P-wave Velocity [km/s] | |
|---|---|---|---|---|
| | A Axis$^1$ | B axis | A axis | B axis |
| C1 | - | - | 5.3 | - |
| C1.1.1 | 15.8 | - | 5.3 | 5.8 |
| C1.1.2 | 15.4 | - | 5.4 | 5.6 |
| C1.2.1 | 17.4 | - | 5.3 | 6.1 |
| C1.2.2 | 13.6 | - | 5.3 | 5.9 |
| C2 | - | 14.4 | 4.9 | 5.3 |
| C3 | - | 13.8 | 5.5 | 5.6 |
| C5 | - | 8.6 | - | - |
| C6.1 | 10.5 | - | - | - |
| C6.2 | 12.9 | - | - | - |
| C7 | 15.2 | - | 4.7 | 5.9 |
| C8 | 13.9 | - | 4.7 | 5.8 |

Figure 5. A cored sample and surface hand sample from Långören Island showing the specimen sections used for indirect Brazilian tensile testing and P-wave velocity measurements. Results from the A axis (vertical) and B axis (horizontal) oriented specimens shown within table.

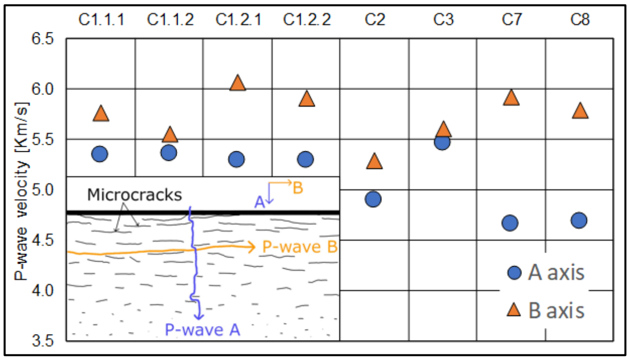

Figure 6. P-wave velocity for samples taken from Långören Island, including those drilled parallel to ground surface.

Prior to indirect tensile testing, the P-wave velocity was measured perpendicular (A axis) and parallel (B axis) to the ground surface (Figure 6). The A axis P-wave velocities are consistently lower than the B axis for the same sample. The A axis velocities were between 5.3 to 5.4 km/s, whereas B axis velocities were more variable, between 5.5 to 6.1 km/s. P-wave values from the core were lowest for sample C2, which lies between the two fracture surfaces and can be projected to the fresh fractures from 2014 (Figure 4). The generally faster B axis over the A axis velocities is consistent with the conceptual orientation of the micro-cracks. In the A axis direction, if micro-cracks are oriented parallel to the ground surface, the wave has to deviate from a straight-line path more than it would in the B axis direction. The more tortuous wave path means that the velocity is slower.

The indirect tensile strength and P-wave velocity measurements indicate a potential preferential orientation to the micro-cracks. However, with so few samples a clear trend with depth is not distinguishable. More samples are necessary in order to clearly determine if the micro-crack density decreases with depth.

### 4.2 Bedrock temperature variations

The preliminary data from the sensors is introduced in Figure 7, where the rock temperature at different depths are plotted. It is clear that the temperature sensor at the shallowest position (0.04 m) shows the largest variation. The temperature of the rock mass in the near surface varies between 35°C and15°C in July and August 2016. On the other hand, sensors at 1.00 m depth show a longer period of fluctuation, with temperatures consistently around 20°C. The temperature at 1.00 m is consistently lower than those sensors located at 0.44 m, however, the evening low air temperatures typically fall below the sub-surface rock temperature. The air temperature is the main driver in the temperature fluctuations, within the superficial layer, but other climatic factors, such as clouds, wind, and even tides (water temperature) could contribute to cooling processes in the area through convection and conduction. The daily variation in the rock temperature profile will be used in the future for model calibration.

The rock temperature is measured at two holes, as previously discussed, to determine any differences between the temperature profile in a fractured and unfractured rock mass. These local variations might change the radiation (heat) absorbed into the rock mass from one location to another and contribute to increased thermal strains in one location over another. There is a significant temperature difference between the near surface (0.04 m) and lower 0.44 sensors as well as an offset in time for the peak temperature (see figure 7). The fracture is acting as an insulator, reducing the amount of

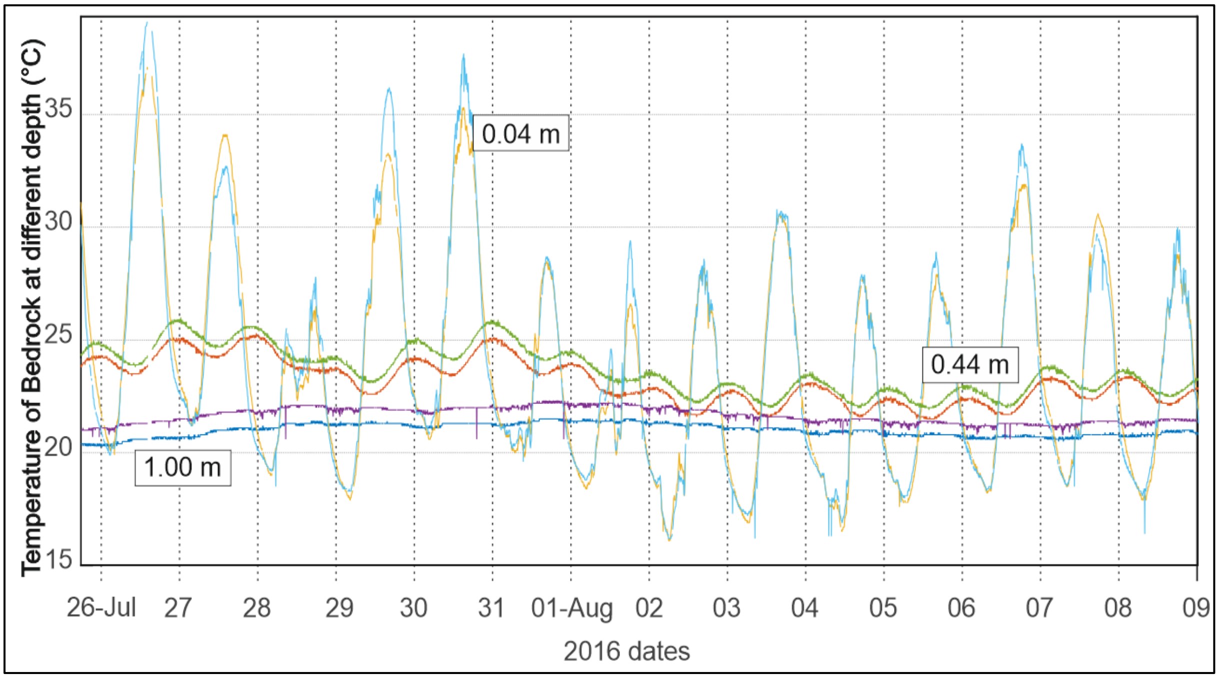

Figure 7: Temperature of bedrock at different depth for Långören Island. Data: July to August 2016 (Leith et al., 2017).

heat flowing from the surface into the rock mass. How this may influence the thermal strain in the near surface could be examined with numerical models in the future.

## 5 CONCLUSIONS

The dynamic fracturing event of 2014 on Långören Island represents a rare opportunity to study fracture growth that is not associated with the typical driving forces, such as gravity or stress change due to excavating. The lack of rain fall or other common climatic drivers and the fact that it was the hottest day on record all point to the potential hazard associated with increasing air temperature on the bedrock stability.

The laboratory data from samples gathered from Långören Island indicate a potential influence of the micro-crack orientation on the tensile strength and P-wave velocity. These micro-cracks represent important sites for continued fracture growth when the stress conditions reach the critical threshold. With substantial influence of the air temperature up to 0.44 m below the ground surface and large thermal changes on daily cycles, there is potential that either the bedrock strength is decreasing with time due to fatigue or that the thermal strain is enough to put the rock mass past the critical fracture growth threshold.

However, more information is needed to better constrain numerical models to aid in understanding the influence of the various potential factors contributing to the formation of micro-cracks and in general fracture growth mechanisms.

The upcoming field season will allow collection of the data from the past year and along with new observations, further advance our understanding of the potential impact of this geo-hazard.

## 6 ACKNOWLEDGEMENT

The author would like to express their gratitude to the Geological Survey of Finland for their initial interest in this fracturing event and sharing data with the research team. Also, many thanks are due to Mr. Sarpaneva and his family, the owner's of Långören Island, for their scientific interest, support during the field work and permission to install the monitoring system. The authors also appreciate the efforts of the reviewer who has helped to improve this paper.

## 7 REFERENCES

Abeka, H., Agyeman, S., and Adom-Asamoah M. 2017. Thermal effect of mass concrete structures in the tropics: experimental, modelling and parametric studies, *Cogent Engineering*, 4: pp18.

Ahjos, T., Saari, J., Penttila, E., and Korhonen, H. 1984. Earthquakes and seismic hazard in Finland. *Engineering Geoogy*. 20: 1-12.

Bakun-Mazor, D., Hatzor, Y.H., Glaser, S.D., and Santamarina, J.C. 2013. Thermally vs. seismically induced block displacements in Masada rock slopes. *International Journal of Rock Mechanics & Mining Sciences*. 61: 196 – 211.

Collins, B.D. and Stock, G.M. 2016. Rockfall triggering by cyclic thermal stressing of exfoliation fractures. *Nature Geoscience*. 9: 395 – 400.

Collins, B.D., Stock, G.M, Eppes, M.C., Lexiw, S.W., Corbett, S.C., and Smith, J.B. 2018. Thermal influences on spontaneous rock dome exfoliation, *Nature Communications*, 9: 11.

Cooper, H.W. and Simmons, G. 1977. The effect of cracks on the thermal expansion of rocks. *Earth and Planetary Science Letters*, 36: 404 – 412.

Edelman, N. 1960. The Gullkrona region, SW Finland. *Geological Survey of Finland, Bulletin,* 187: 1 – 92.

Edelman, N. and Jaanus-Järkkälä, M. 1983. A plate tectonic interpretation of the Precambrian of the Archipelago of southwestern Finland. *Geological Survey of Finland, Bulletin,* 325: 1 – 33.

Granö, O., Roto, M., and Laurila, L. 1999. Environment and land use in the shore zone of the coast of Finland. *Institute of Geography, University of Turku.* 160: 1 – 76.

Greif, V., Sassa, K., and Fukuoka, H. 2006. Failure mechanism in an extremely slow rock slide at Bitchu-Matsuyama castle site (Japan). *Landslides*. 3: 22 – 38.

Hall, K. and Andre, M.F. 2001. New insisghts into rock weathering from high-frequency rock temperature data: an Antartic study of weathering by thermal stress. *Geomorphology.* 41: 23 – 35.

Hoek, E. and Martin, C.D. 2014. Fracture initiation and propagation in intact rock – A review. *Journal of Rock Mechanics and Geotechnical Engineering.* 6(4): 287-300.

Huang, X., Tang, C.A., Tang, S.B., Xiw, L.M. 2017. Numerical Test of Thermal Cracking Behaviour in a Nuclear Waste Disposal, 4th *ISRM Young Scholars Symposium on Rock Mechanics,* International Society for Rock Mechanics and Rock Engineering, Jeju, South Korea, 4: 10-13.

ISRM, 1978. Suggested methods for determining tensile strength of rock materials. *Int J Rock Mech Min Sci Geomech Abstr,* 15(3):99–103.

Jansen, D.P., Carlson, S.R., Young, R.P., and Hutchins, D.A. 1993. Ultrasonic Imaging and Acoustic Emission Monitoring of Thermally Induced Microcracks in Lac du Bonnet Granite. *Journal of Geophysical Research.* 98: 231 – 243.

Johansson, J.M., Davis, J.L., Scherneck, H.G., Milne, G.A., Vermeer, M., Mitrovica, J.X., Bennett, R.A., Jonsson, B., Elgered, G., Elosegui, P., Koivula, H., Poutanen, M., Ronnang, B.O., and Shapiro, I.I. 2002. Continuous GPS measurements of postglacial adjustment in Fennoscandia. *Journal of Geophysical research*. 107(3): 1-28.

Jokinsen, H. 2010. Major potentially climate induced changes in the coastal ecosystem of the western Gulf of Finland – a review. *University of Helsinki, Vaccia.* 5: 1 – 30.

Kaskela, A. 2017. Seabed landscapes of the Baltic Sea: Geological characterization of the seabed with spatial analysis techniques. Ph.D. thesis, University of Helsinki (Finland).

Lamp, J.L., Marchant, D.R., Mackay, S.L., and Head, J.W. 2017. Thermal stress weathering and the spalling of Antarctic rocks, *Journal of Geophysics Research: Earth Surface*. 122: 3 – 24.

Leith, K., Perras, M., Siren, T., Rantanen, T., Heinonen, S., and Loew, S. 2017. Dynamic fracture development in response to extreme summer temperatures: 27/7/2014, Långören Island, Finland. *19th EGU General Assembly,* EGU2017, Vienna, Austria4:1.

Leith, K., Perras, M.A., Siren, T., Rantanen, T., Wolter, A., and Loew, S. 2017. Development of a new thermally-induced fracture in a 12,000 year old bedrock surface. In Proc. Progressive Rock Failure Conference, Ascona, Switzerland.

Paulamäki, S., Paananen, M., and Elo, S. 2002. Structure and geological evolution of the bedrock of southern Satakunta SW Finland. *Geological Survey of Finland, Possiva 2002*, 4: 1 – 128.

Pennala, J. 2017. Update of Finnish in situ Rock Stress Data. Master thesis, Aalto University (Finland).

Poutanen, M., Dransch, D., Gregersen, S., Haubrock, S., Ivins, E.R., Kleman, V., Kozlovskaya, E., Kukkonen, I., Lund, B., Lunkka, J.P., Milne, G., Muller, J., Pascal, C., Petterson, B.R., Scherneck, H.G., Steffen, H., Vermeersen, B., and Wold, D. 2010. Upper mantle dynamic and quaternary climate in cratonic areas (DynaQlim) – Understanding the glacial isostatic adjustment. *Journal of Geodynamics*. 50 (1): 2 – 7.

Rantanen, T. 2016. Rock Mechanics analyses of exfoliation fractures at Långören Island. Master thesis, Aalto University (Finland).

Rice, J.R. 1978. Thermodynamics of the quasi-static growth of Griffith cracks, *Journal of Mechanic Physics Solid*, 26: 67-78.

Saari, J. 2000. Seismic activity parameters of the Finnish potential repository sites. *Geological Survey of Finland, Possiva 2000*, 13: 1 – 39.

Sih, G.C. and DiTommaso, A. 1985. *Fracture mechanics of concrete: Structural application and numerical calculation,* 1st ed., Martinus Nijhoff Publishers, Dordrecht, Netherlands.

Vlcko, J., Greif, V., Grof, V., Jezny, M., Petro, L., and Brcek, M. 2008. Rock displacement and thermal expansion study at historic heritage sites in Slovakia. *Environmental Geology.* 58: 14.

Virtasalo, J.J. 2006. Late-Weichselian – Flandrian Depositional History of the Archipelago Sea, northern Baltic Sea. *Annales University of Turku*, 196: 1 – 156.